Accelerator Division

ESS AD Technical Note
ESS/AD/0021

Lali Tchelidze

Design of the ESS Main Beam Loss Detector

12 September 2011

A technical report on the

DESIGN OF THE ESS MAIN BEAM LOSS DETECTOR

(A detailed description of calculations presented in IPAC'11 paper)

by

Lali Tchelidze*

European Spallation Source ESS AB

P.O. Box 176, SE-221 00 Lund, Sweden

*Contact: lali.tchelidze@esss.se

Abstract

This report is a summary of the detailed calculations for designin the ESS main loss detector. It starts with describing the ESS project and the proton accelerator. Then, the general requirements for the loss detectors are listed. Based on these requirements few detectors are chosen. The main loss detector is chosen to be a cylindrical ionization chamber and a new design is given based on the time response calculations.

The new prototype detector response functions are calculated using the MARS and Geant4 particle transport codes.The response functions are simulated for different particle types, energies and incident angle.

Contents

Chapter 1

Overview of the ESS Project

The european spallation source will be an accelerator complex consisting of a 5 MW proton accelerator, target and a number of neutron instruments. ESS will be built in Lund, Sweden. The facility will be the world's most intense spallation neutron source for neutron scattering research. In Fig. 3.3 the schematic view of the accelerator is given. The accelerator is divided into the normal conducting and superconducting parts. Protons are generated in the ion source and after passing through the low energy beam transport (LEBT) they are accelerated to 3 MeV in the radio frequency quadrupole (RFQ). Later, the proton beam is injected in a medium energy beam transport (MEBT) and a drift tube linac (DTL) further accelerates the beam up to 50 MeV. The beam continues to travel through the superconducting part of the machine, where the acceleration is done by the superconducting radio-frequency (SRF) technology, and at the end of the journey the protons achieve 2.5 GeV kinetic energy. After passing through the high energy beam transport (HEBT), the beam hits the target [1].

The ESS accelerator will be around 500 m long and will generate 2.86 ms long macro pulses, with an average pulse current of 50 mA and 14 Hz repetition rate, resulting in a maxim beam power of 5 MW [1].

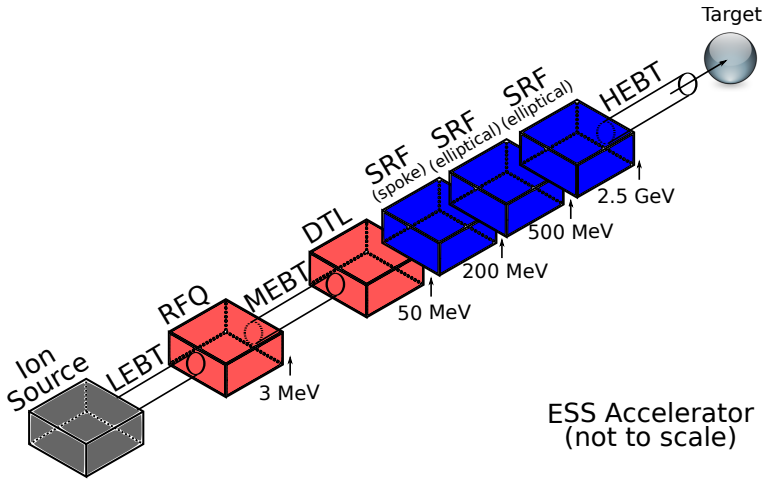

Figure 1.1: Schematic view of the ESS accelerator.

Chapter 2

ESS Beam Loss Monitoring System Requirements

2.1 General Requirements

According to the baseline parameters, ESS will generate 1.83×10^{15} protons in a single macro-bunch. However, the BLM system will be designed for an intensity of 2.7×10^{15} (1.5 times greater than the baseline value) to allow the possible future power upgrades.

The BLM system has the following requirements. It should provide real time data to tune the beam and minimize losses. It should measure the losses continuously and also should be able to quickly send the beam halt signal to the machine protection system in case the losses ecxeed the limits. There will be several thresholds set to inhibit the beam. One threshold will be set for average long time losses according to the allowed activation levels in the machine and the tunnel. Another limit will be set for an uncontrolled, high losses based on the calculations partially presented in the further sections.

2.2 Sensitivity requirements

The BLM system detectors should be sensitive enough to observe low and slow signals as well as fast and high signals. Sensitivity of 70 nC/Rad was obtained with an Argon filled, sealed glass ionization chamber designed and developed by Shafer at Fermi National Accelerator Lab (FNAL) [2]. The same sensitivity was kept for the spallation neutron source (SNS) main BLM detector [3]. SNS is a similar to ESS accelerator and produces a pulsed H^- beam of up to 1.4 MW [3]. Although higher sensitivity is desired, the 70 nC/Rad is thought to be good enough for the ESS as well. Futher tests will determine if there is a need for the sensitivity increase.

2.3 Time response requirements

In terms of the response time, the main requirement for the beam loss detector is the following: even in the case of full power loss, it should generate a beam abort signal fast enough to prevent any damage. At SNS the BLM system was designed so that it can produce stop-the -beam signal in less than 10 μs [4]. Since ESS has roughly 3-5 times higher power the required response time has to be rescaled by the same factor. This means that a new, faster detector has to be designed which will respond to critical losses in less than 2-3 μs. The new prototype design is given in the next section. The future simulations and tests will verify the goodness of the prototype.

2.4 Dynamic range requirements

Like at SNS we require the BLM system to be able to measure at most 1 % of local beam loss and achieve at least 1 % resolution of 1 W/m loss limit [3]. This implies dynamic range of 10^6-10^7. This is achievable with the current ionization chamber detectors and subsequent electronics circuits [4].

Chapter 3

The Detector

3.1 Choice of detector

The list below shows several detector candidates for loss monitors, compared to an ionization chamber:

- secondary emission monitor: very low sensitivity (10^{-5} IC);
- PIN photodiodes: sensitivity 0.1 IC, even worse for neutrons;
- scintillator-photomultiplier tubes: very good sensitivity (>10 IC) and good time response. Moderate radiation hardness. However, the gain instabilities require excessive reliability maintenance;
- IC: large dynamic range, very good stability, time response 500 ns. Very good radiation hardness, reasonable sensitivity.

As at most of the hadron accelerators, we chose ionization chamber to be the ESS main loss detector. It is cheap and requires very low maintancence.

3.2 Design of a detector

Now, we need to design a cylndrical coaxial ionization chamber that meets the requirements. We would like to keep the same sensitivity as in the

original FNAL designed ionization chamber (the sensitivity was also kept at the SNS), but as mentioned above we need to decrease the response time of the detector by a factor of 3-5.

The positive ion transit time in an ionization chamber is given by [6]

$$t = \frac{d^2}{\mu_0 V (P_0/P)} \tag{3.1}$$

where μ_0 is the ion mobility at standard temperature and pressure, V is applied voltage, P_0 is an atmospheric pressure, P working pressure and d is an effective electrode separation. For cylindrical geometry the effective hap between the electrodes

$$d^2 = \frac{1}{2}\left(R^2 - r^2\right)\left(\ln(R/r)\right)) \tag{3.2}$$

where R and r are the outer and inner radii of the electrodes respectively. As already mentioned few times, both at FNAL and SNS cylindrical ionization chambers are used. The same volume of $110\,\mathrm{cm}^3$ Argon gas is used in both detectors at the same pressure. Only the dimensions have been changed from the FNAL to SNS design to decrease the ion transit time. The FNAL detector dimensions were: $2R_{FNAL} = 1.5\,\mathrm{inch}$, $2r_{FNAL} = 0.25\,\mathrm{inch}$, lenght of the detector $L_{FNAL} = 4\,\mathrm{inch}$. This dimensions were changed to $2R_{SNS} = 1.5\,\mathrm{inch}$, $2r_{SNS} = 1\,\mathrm{inch}$, $L_{SNS} = 6.7\,\mathrm{inch}$,resulting in the same sensitive volume and sensitivity of the detector, and considerably decreasing the collection time. The collection time measured for FNAL were $t_{FNAL}(@V = 2\mathrm{kV}) = 700\mu s$ and $t_{FNAL}(@V = 3\mathrm{kV}) = 560\mu s$. This figure was decreased to $t_{SNS}(@V = 3\mathrm{kV}) = 72\mu s$.

We, at ESS chose the same gas, Argon (Argon was initially chosen to increase the ion mobilities [7]) at the same conditions and plotted the ion transit time as a function of the inner electrode radius, for fixed outer electrode radius of R =4 cm and voltage V =3 kV. The results are shown in the

figure below.

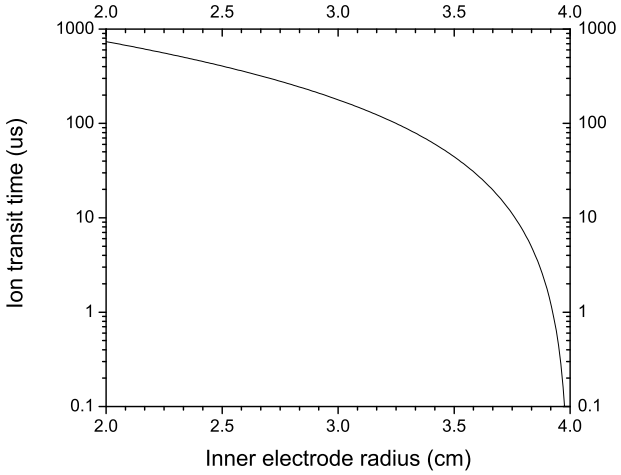

Figure 3.1: Cylindrical ionization chamber ion collection time as a function of the inner cylinder radius. The detector is filled with Argon gas at 1 atm pressure. Outer electrode radius is 4 cm, bias voltage - 3 kV and effective volume - 110 cm^3.

Choosing the inner electrode radius to be r =3.8 cm and length of the detector 23 cm will decrease the ion transit time to less than 8 μs, leaving the sensitivity unchanged. The design of the detector is shown below.

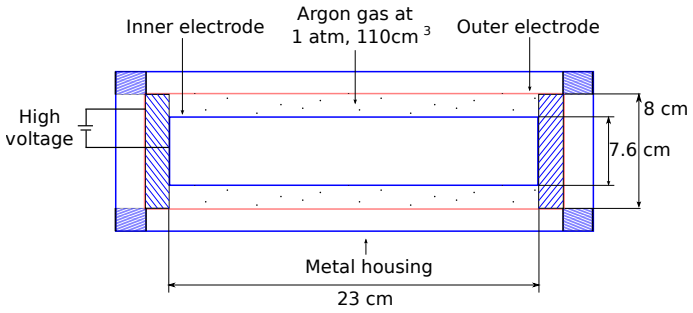

Figure 3.2: ESS prototype ionization chamber.

3.2.1 Breakdown voltage for the Argon gas

The short gap in between the electrodes rises the question about the maximum voltage one can safely apply to them. The figure below shows meausred values of the gas breakdown voltage for different gasses - the so called Paschen curves [11]. The Argon gas in our detector is at $1 - 1.1\,\mathrm{atm} \approx 800\,\mathrm{Torr}$, the length of the gap where the gas is inclosed is 2 mm, so $P \cdot d \approx 160\,\mathrm{Torr{\cdot}cm}$. This results in approximately 4 kV as for the breakdown voltage. Since we plan to operate at 3 kV, it should be safe to use the detector.

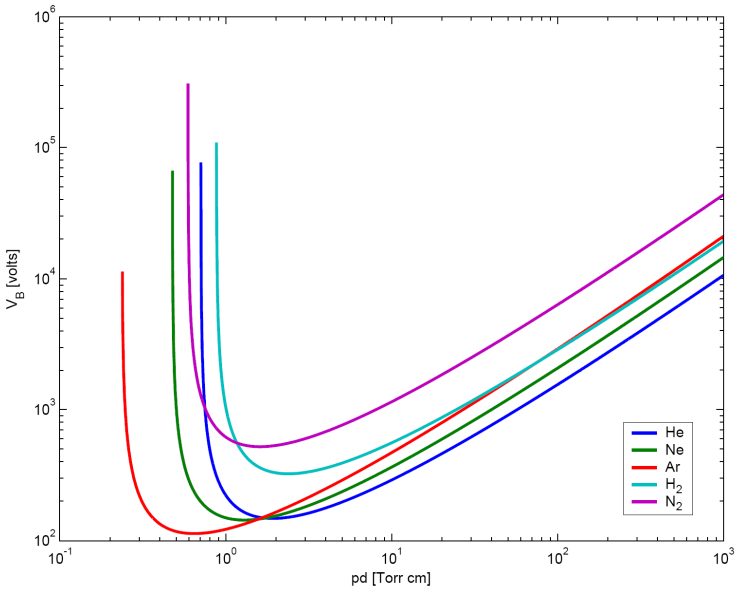

Figure 3.3: Paschen curves for the gas breakdown voltage for different gasses .

Chapter 4

The new ionization chamber response functions

Detector response function simulations were performed using the particle transport code MARS [8, 9]. The response functions of the Argon gas of the detector were calculated for different incident particles, energies and angles. In Fig. 4.1 the plot is given for zero incident angle.

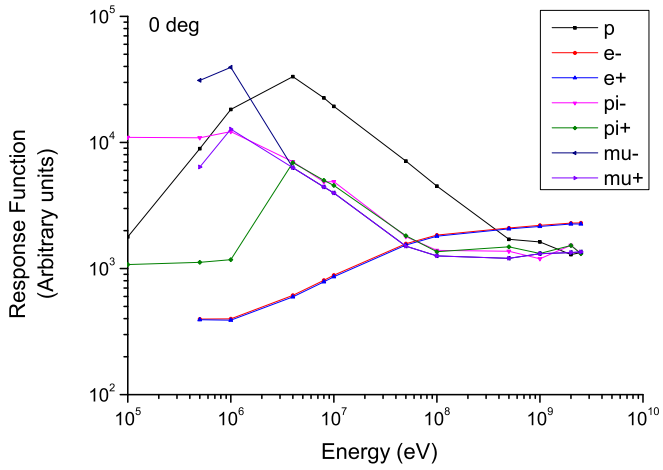

Figure 4.1: ESS prototype ionization chamber response function as a function of incident particle type and energy. For zero incident angle.

The input files MARS.INP, GEOM.INP and XYZHIS.INP look the following way:

MARS.INP - the main input file

```
Name of the file
/opt/mars/mars15/dat
INDX T T T
CTRL 1
C TYPE 18
NEVT 1000000
ENRG 0.01
INIT 0. 0. 5. 0. 0. 1.
IPIB 1 1
BEAM 4. 4.
NLNG 3
ZSEC 5. 28. 33. 2501 = 0 0 0
RSEC 10.
NMAT 5
MATR 'WATR' 'AIR' 'STST' 'CU' 'AR'
ICEM 4=1
NOBL 1
RZOB 0. 10. 5. 28.
STOP
```

GEOM.INP - the geometry input file

```
Extended geometry file
cyl1 2 0 5 0. 0. 5. 3.8 4. 23.
```

cyl2 2 0 0 0. 0. 5. 0. 3.8 23.

stop

VNAME TYPE TRF IM X0 Y0 Z0 C1 C2 C3 NZ NR

XYZHIS.INP - the histogramming input file

XYZ histograms

xyz 3.8 4. -0.1 0.1 5. 28. 1 1 3 XZ-scan

PDT PDP PDN PDK PDM PDG PDE

stop

STA DRE FLT FLP FLN FLN>0.02 FLK FLM>0.1 FLG FLE DAB DPA

DET DET>0.02 DEP DEN DEK DEM DEG DEE

PDT PDP PDN PDK PDM PDG PDE DPH HYD HEL TRI

C STA- star density E>50 MeV (cm^{-3} s^{-1})

C DRE- residual dose on contact (mSv/hr)

C FLT- total flux of hadrons E>ETFT (cm^{-2} s^{-1})

C FLP- flux of protons E>ETFH (cm^{-2} s^{-1})

C FLN- flux of neutrons E>ETFN (cm^{-2} s^{-1})

C FLK- flux of pions/kaons E>ETFH (cm^{-2} s^{-1})

C FLM- flux of muons E>ETFM (cm^{-2} s^{-1})

C FLG- flux of photons E>ETFG (cm^{-2} s^{-1})

C FLE- flux of e-e+ E>ETFE (cm^{-2} s^{-1})

C

C DAB- absorbed dose (Gy/yr) at 2.e7 s/yr

C DPA- DPA, total (recoil+NIEL+neut+EMS) (DPA/yr) at 2.e7 s/yr

C DPH- DPA, NIEL hadrons and muons (DPA/yr) at 2.e7 s/yr

C DPN- DPA, neutrons at E ¡ 14 MeV (DPA/yr) at 2.e7 s/yr

C DPE- DPA, EMS (DPA/yr) at 2.e7 s/yr

C HYD- Hydrogen production (cm^{-3} s^{-1})

C HEL- Helium production (cm^{-3} s^{-1})

C TRI- Tritium gas production (cm^{-3} s^{-1})

C

C DET- FTD prompt dose equivalent, total (mSv/hr)

C DEP- FTD prompt dose equivalent, proton (mSv/hr)

C DEN- FTD prompt dose equivalent, neutron (mSv/hr)

C DEK- FTD prompt dose equivalent, pi/K (mSv/hr)

C DEM- FTD prompt dose equivalent, muon (mSv/hr)

C DEG- FTD prompt dose equivalent, photon (mSv/hr)

C DEE- FTD prompt dose equivalent, e+e- (mSv/hr)

C

C PDP- power density, proton (mW/g or Gy/s)

C PDN- power density, neutron (mW/g or Gy/s)

C PDK- power density, pion/kaon (mW/g or Gy/s)

C PDM- power density, muon (mW/g or Gy/s)

C PDG- power density, photon (mW/g or Gy/s)

C PDE- power density, e-e+ (mW/g or Gy/s)

C

C SPP- proton energy spectrum (GeV^{-1} cm^{-2} s^{-1})

C SPN- neutron energy spectrum (GeV^{-1} cm^{-2} s^{-1})

C SPK- pion/kaon energy spectrum (GeV^{-1} cm^{-2} s^{-1})

C SPM- muon energy spectrum (GeV^{-1} cm^{-2} s^{-1})

C SPG- photon energy spectrum (GeV^{-1} cm^{-2} s^{-1})

C SPE- e+e- energy spectrum (GeV^{-1} cm^{-2} s^{-1})

C

Bibliography

[1] http://esss.se/linac/Parameters/High_Level.pdf aceessed on July 28th, 2011

[2] R. E. Shafer, R. E. Gerig, A. E. Baumbaugh and C. R. Wegner, "The Tevatron Beam Position and Beam Loss Monitoring Systems", Proc. 12th Int'l Conf. on High Energy Accel., FNAL, 1983

[3] R. Witkover and D. Gassner, 10th Beam Instrumentation Workshop, BNL, NY, May 6-9, 2002. BNL-69257

[4] D. Gassner, P. Cameron, C. Mi and R. Witkover, "Spallation Neutron Source Beam Loss Monitor System", PAC'03, p. 2447

[5] Cern Accelerator School lecture notes by K. Wittenburg: http://cas.web.cern.ch/cas/France-2008/Lectures/Wittenburg-BLM.pdf

[6] R. L. Witkover, D. Gassner, "Design and Testing of the New Ion Chamber Loss Monitor for SNS", PAC'03, p. 2450.

[7] M. Plum and D. Brown, "Response of Air-Filled Ion Chambers to high Intensity Radiation Pulses", PAC'98, p. 2181.

[8] N. V. Mokhov, "The Mars Code System User's Guide", Fermilab-FN-628, 1995

[9] N. V. Mokhov, S. I. Striganov, AIP Conf. Proc. 896, pp. 50-60, 2007

[10] A. Jansson, L. Tchelidze, H. Danared, M. Eshraqi, "Beam Instrumentation for the European Spallation Source", PAC'11, New York, NY, USA

[11] M. A. Lieberman, A. J. Lichtenberg, "Principles of Plasma Discharges and Materials Processing", Wiley 2005.